Stop and other searches

Caroline Collard for the ATLAS and CMS Collaborations

IPHC, CNRS/IN2P3, 23 Rue du Loess, BP28, 67037 Strasbourg Cedex 2, France

DOI: http://dx.doi.org/10.3204/DESY-PROC-2014-02/40

The latest results from LHC on direct pair production of third-generation squarks are reviewed. We present searches performed for different decay modes of stop and sbottom using the full set of 8 TeV LHC data recorded in 2012 (corresponding to 20/fb).

1 Introduction

The search for the third-generation squarks, namely the stop $\tilde{t}_1$ and sbottom $\tilde{b}_1$, is of particular interest in the frame of Natural SUSY which tends to accommodate a Higgs boson of 125 GeV. Stop and sbottom can be produced directly by pair through the $pp \to \tilde{t}_1\tilde{t}_1^*$ and $pp \to \tilde{b}_1\tilde{b}_1^*$ processes, with a cross section rapidly falling with an increasing value of their mass ($m_{\tilde{t}_1}$ or $m_{\tilde{b}_1}$) [1]. If the gluino is not too heavy to be produced at the LHC, the gluino-mediated production mode is also possible, and in that case, is dominant.

The analyses performed on the subject by the ATLAS [2] and CMS [3] Collaborations are done mainly in the frame of R-parity conservation (RPC), which implies that SUSY particles are pair-produced and decay up to the lightest supersymmetric particle (LSP). As the LSP is stable, it provides a clear signature in the detector by a large missing transverse energy (MET). In contrast, for R-parity violation (RPV), the LSP will decay into Standard Model (SM) particles leading to final states of larger multiplicity and without significant MET.

In all analyses, a strong effort is put on validating and estimating the SM contributions with data-driven methods. The absence of deviation in the data with respect to the SM processes leads up to now to the extraction of exclusion limits. Simplified models of Supersymmetry (SMS) are commonly used to set such limits on specific SUSY processes, as they allow describing a process with a limited set of free parameters, typically the masses of the SUSY particles which appear in the process. They also assume a branching ratio (BR) to a dedicated decay mode of 100%.

We present here only the most recent results for direct pair production of $\tilde{t}_1$ or $\tilde{b}_1$, assuming RPC, based on the full 2012 data set corresponding to an integrated luminosity of $\sim$20/fb.

2 Search for sbottom decaying into a bottom quark and the lightest neutralino

The study of the $\tilde{b}_1 \to b\tilde{\chi}_1^0$ process with the lightest neutralino $\tilde{\chi}_1^0$ as LSP has been performed [4] by ATLAS. The events are selected with 0 lepton, 2 jets identified as originating from a b quark ("b-tagged jets") and MET>150 GeV in the final state and categorized into two signal regions.

The first signal region is defined for large mass differences $\Delta m(\tilde{b}_1, \tilde{\chi}_1^0)$ between the $\tilde{b}_1$ and the $\tilde{\chi}_1^0$, with a veto on any additional jet. It makes use of the contransverse mass m_{CT} displayed on Fig. 1 (left):

$$m_{CT}^2(v_1, v_2) = [E_T(v_1) + E_T(v_2)]^2 - [p_T(v_1) - p_T(v2)]^2 \quad (1)$$

which tends to reconstruct the mass of a heavy particle, pair-produced and decaying semi-invisibly, from the information on the two visible particles (v_1 and v_2, i.e. the b-tagged jets here). To consider also smaller mass differences $\Delta m(\tilde{b}_1, \tilde{\chi}_1^0)$ (≤ 100 GeV), a second signal region is defined, asking for a leading jet coming from an initial state radiation (ISR) not b-tagged, the b-tagging criteria being only applied on the 2^{nd} and 3^{rd} jets.

As the data in these two signal regions are in agreement with the expected SM predictions, exclusion limits are extracted. They extends considerably the previous results from Tevatron [5, 6] as displayed on Fig. 1 (right) in the 2D plane $m_{\tilde{\chi}_1^0}$ vs $m_{\tilde{b}_1}$: $m_{\tilde{b}_1}$ up to 620 GeV are excluded at 95% of confidence level (CL) for $m_{\tilde{\chi}_1^0}$ <120 GeV; and $\Delta m(\tilde{b}_1, \tilde{\chi}_1^0)$ >50 GeV are excluded up to $m_{\tilde{b}_1}$ of 300 GeV.

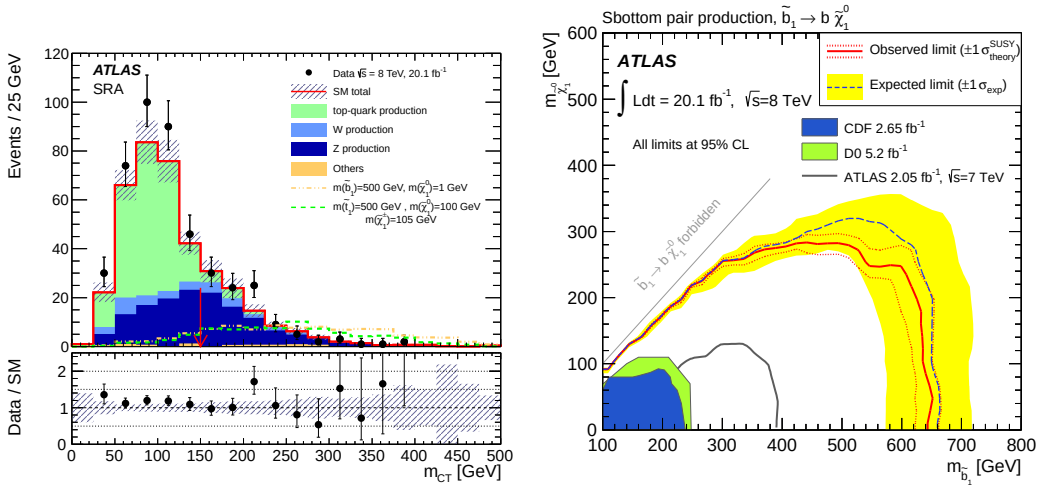

Figure 1: Left: Distribution of m_{CT}. The different backgrounds are represented by colored histograms, the shaded band includes statistical, detector-related and theoretical systematic uncertainties. For illustration the distributions expected for two signal models are displayed. Right: Exclusion limits at 95% CL in the $(m_{\tilde{b}_1}, m_{\tilde{\chi}_1^0})$ plane for the $\tilde{b}_1 \to b\tilde{\chi}_1^0$ process. Previous results from Tevatron are also shown.

3 Search for sbottom decaying into a top quark and the lightest chargino

The $\tilde{b}_1 \to t\tilde{\chi}_1^{\pm}$ process is studied by CMS with an event selection based on the presence of 2 leptons of same sign and at least two jets [7]. A veto on events with a third lepton is applied,

if this lepton is identified as coming from the Z decay. This analysis defines multiple signal regions, with different requirements on the jet multiplicity, the scalar sum H_T of the transverse momenta of the jets, the b-tagged jet multiplicity and MET, to maximize the sensitivity to many models. No excess with respect to the SM predictions is observed and the results are therefore interpreted in the frame of $\tilde{b}_1 \to t\tilde{\chi}_1^{\pm}$, with $\tilde{\chi}_1^{\pm} \to W\tilde{\chi}_1^0$, depending on the mass of the 3 SUSY particles. Figure 2 (left) shows the 95% CL exclusion limits in the 2D plane $m_{\tilde{\chi}_1^{\pm}}$ vs. $m_{\tilde{b}_1}$ for $m_{\tilde{\chi}_1^0}$= 50 GeV and Fig. 2 (right) presents these limits as a function of $m_{\tilde{\chi}_1^0}$ and $m_{\tilde{b}_1}$ for the mass hierarchy $m_{\tilde{\chi}_1^0}/m_{\tilde{\chi}_1^{\pm}} = 0.5$. A similar analysis has been performed by ATLAS, leading to similar results [8].

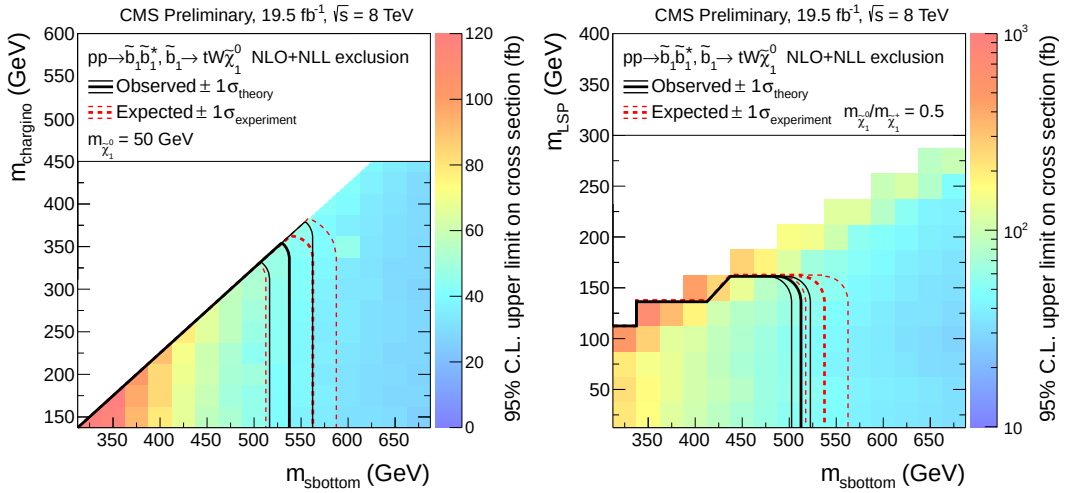

Figure 2: Exclusion regions at 95% CL for the $\tilde{b}_1 \to t\tilde{\chi}_1^{\pm}$ process, in the 2D planes (left) $m_{\tilde{\chi}_1^{\pm}}$ vs. $m_{\tilde{b}_1}$ for $m_{\tilde{\chi}_1^0}$= 50 GeV and (right) $m_{\tilde{\chi}_1^0}$ vs. $m_{\tilde{b}_1}$ for $m_{\tilde{\chi}_1^0}/m_{\tilde{\chi}_1^{\pm}} = 0.5$.

4 Search for stop decaying into a charm quark and the lightest neutralino

The search of the $\tilde{t}_1 \to c\tilde{\chi}_1^0$ decay mode performed by ATLAS is only feasible in presence of an ISR jet, in order to identify the signal events from the large multijet background [9]. For small values of $\Delta m(\tilde{t}_1, \tilde{\chi}_1^0)$, the monojet signature is designed, requesting a leading ISR jet of transverse momentum p_T >280 GeV, a low jet multiplicity (≤3) and MET>220 GeV. For moderated values of $\Delta m(\tilde{t}_1, \tilde{\chi}_1^0)$ ($\sim$ 20 to 80 GeV), the selection uses a c-tagging technique to identify jet originating from a c quark, which is based on a MVA algorithm using information from the impact parameters of displaced tracks and on secondary and tertiary decay vertices. In addition to a cut on MET>410 GeV, at least 4 jets are requested for this c-tagged signature. The leading jet with p_T >270 GeV coming from ISR is not tagged, a b-veto is applied on the 2^{nd} and 3^{rd} jets and the c-tagging is applied on the 4^{th} jet for which the discriminant is presented on Fig. 3 (left).

These two signatures do not present any excess in the data with respect to the SM expectations. The limits extracted in the $(m_{\tilde{t}_1}, m_{\tilde{\chi}_1^0})$ plane are shown on Fig. 3 (right): $m_{\tilde{t}_1}$ up to 200 GeV are excluded at 95% CL for $\Delta m(\tilde{t}_1, \tilde{\chi}_1^0) < 85$ GeV; $m_{\tilde{t}_1}$ up to 230 GeV are excluded for $m_{\tilde{\chi}_1^0}$ =200 GeV. This extends significantly previous results from Tevatron [10, 11] and LEP [12] experiments.

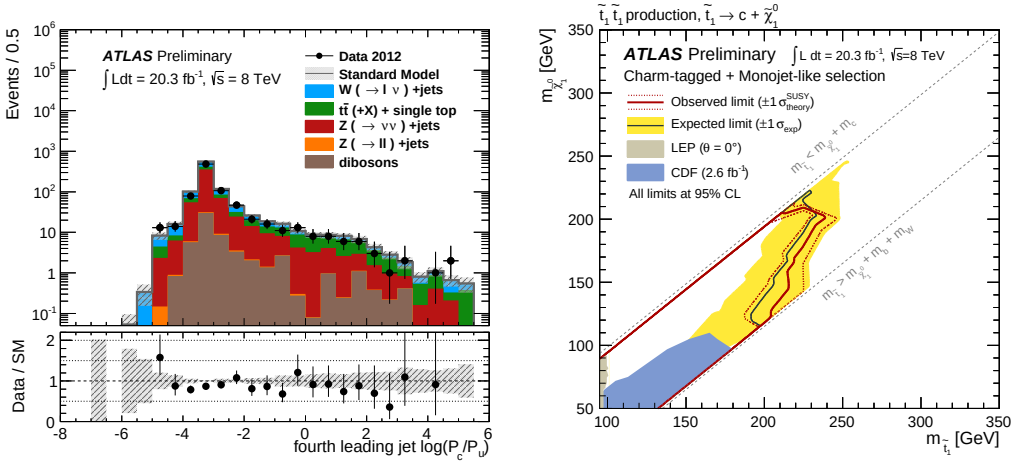

Figure 3: Left: Distribution for the 4^{th} leading jet, of the discriminator against jet identified as originating from a light parton. Data are compared to MC simulations for the different SM processes, the error band includes the statistical and experimental uncertainties in the predictions. Right: Exclusion plane at 95% CL as a function of $m_{\tilde{t}_1}$ and $m_{\tilde{\chi}_1^0}$ for the $\tilde{t}_1 \to c\tilde{\chi}_1^0$ process. Results from previous experiments are also displayed.

5 Search for stop decaying into a top quark and the lightest neutralino

The razor analysis [13] performed by CMS tends to estimate the mass scale of a process when moving from the lab frame to the frame in which particles are clustered into two "mega" jets of same momentum. The razor variables are defined as

$$M_R \equiv \sqrt{(p^{j_1} + p^{j_2})^2 - (p_z^{j_1} + p_z^{j_2})^2}\,,$$
$$M_T^R \equiv \sqrt{\frac{\mathrm{MET}(p_T^{j_1} + p_T^{j_2}) - \vec{\mathrm{MET}}\cdot(\vec{p}_T^{\,j_1} + \vec{p}_T^{\,j_2})}{2}}\,. \qquad (2)$$

M_R depends only on the momenta $\vec{p}^{\,j_i}$ of the 2 mega jets (j_1 and j_2), with p^{j_i} being the absolute value of the 3-momentum of the i^{th} jet and $p_z^{j_i}$ ($p_T^{j_i}$) its longitudinal (transverse) component, whereas the transverse variable M_T^R depends also on MET. Figure 4 shows how SUSY signal (top left) differs from SM background (top right) in the plane $R^2 = (\frac{M_T^R}{M_R})^2$ versus M_R.

The final states, which contain 0 or 1 lepton and at least 1 b-tagged jet, are used for the search, they are separated into categories depending on the lepton and jet multiplicities. In

each category, the background is estimated from a 2D fit on R^2 and M_R in side-band regions (low M_R or low R) as shown on Fig. 4 (bottom) and extrapolated to the search region.

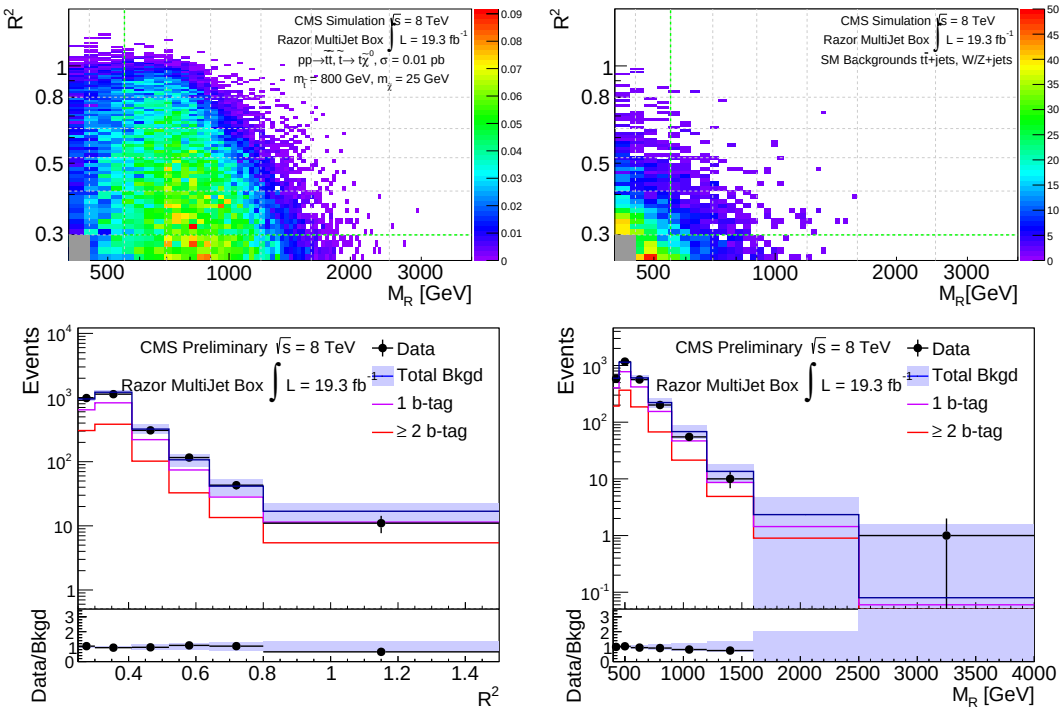

Figure 4: Top: Event distribution in the (M_R, R^2) plane for (left) the $\tilde{t}_1 \to t\tilde{\chi}_1^0$ signal and (right) the SM processes. Bottom: Projection of the sideband fit result on R^2 (left) and M_R (right). The separate background contributions from 1 b-tagged jet and ≥ 2 b-tagged jets are also shown.

No deviation is observed in any category, allowing to exclude at 95% CL $m_{\tilde{t}_1}$ between 340 and 740 GeV for light $\tilde{\chi}_1^0$ as presented on the left part of Fig. 5. This analysis is complementary to the search [14] from CMS which extends the exclusion limits to lower values of $\Delta m(\tilde{t}_1, \tilde{\chi}_1^0)$.

The right part of Fig. 5 shows the exclusion limits obtained by ATLAS. New results [15] based on a selection of two leptons of opposite sign and at least two jets, complete the previous measurements with 0 lepton [16] and 1 lepton [17] in the final state with 8 TeV LHC data.

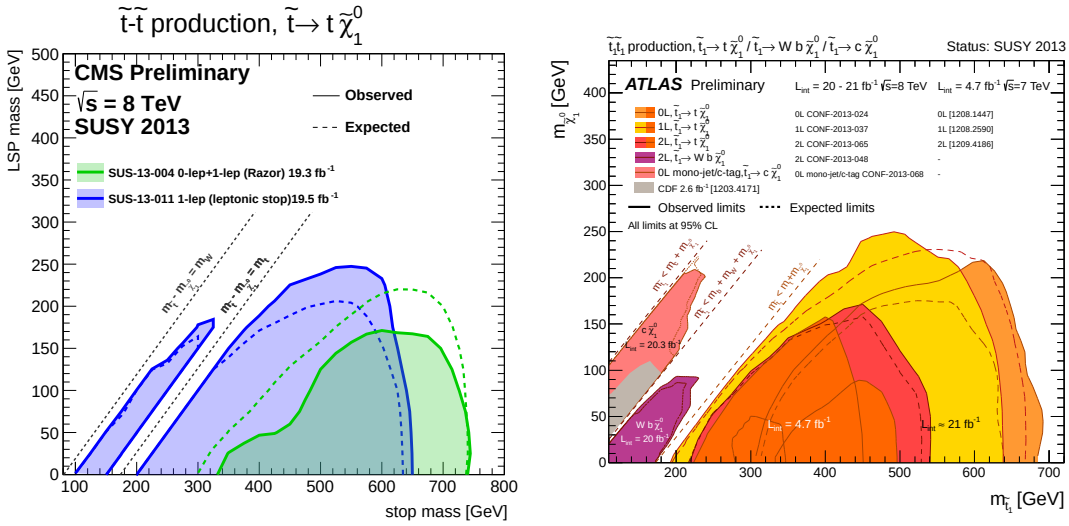

Figure 5: Summary of exlcusion limits obtained by CMS (left) and ATLAS (right) with $\tilde{t}_1 \to t\tilde{\chi}_1^0$ searches, in the plane $m_{\tilde{\chi}_1^0}$ versus $m_{\tilde{t}_1}$.

6 Search for stop decaying into a bottom quark and the lightest chargino

The search by ATLAS for $\tilde{t}_1 \to b\tilde{\chi}_1^\pm$ with $\tilde{\chi}_1^\pm \to W\tilde{\chi}_1^0$, with 2 leptons of opposite sign and at least 2 b-tagged jets selected in the final state [15], makes use of the stransverse mass:

$$m_{T2}(p_T^1, p_T^2, q_T) = \min_{q_T^1+q_T^2=q_T} \left\{ max\left[m_T(p_T^1, q_T^1), m_T(p_T^2, q_T^2) \right] \right\}$$
$$\text{with } m_T(p_T^1, p_T^2) = \sqrt{2|p_T^1||p_T^2|(1-\cos(\Delta\phi))} \qquad (3)$$

where p_T^1 and p_T^2 are the transverse momenta of 2 particles separated in the transverse plane by an angle $\Delta\phi$. The minimization for $m_{T2}(p_T^1, p_T^2, q_T)$ is performed over all the possible decompositions of q_T in the q_T^1 and q_T^2 vectors such as $q_T^1 + q_T^2 = q_T$.

The m_{T2} variable can be constructed from the two leptons and MET as in [18], such as $m_{T2}(\ell_1, \ell_2, \text{MET})$ is bounded at m_W for the $t\bar{t}$ and WW processes and is correlated to $\Delta m(\tilde{\chi}_1^\pm, \tilde{\chi}_1^0)$ for the $\tilde{t}_1\tilde{t}_1^*$ signal, providing interest for the region with large $\Delta m(\tilde{\chi}_1^\pm, \tilde{\chi}_1^0)$.

On the contrary, in [15], the m_{T2} variable is constructed using also the momenta of the b-tagged jets: $m_{T2}(b_1, b_2, \ell_1 + \ell_2 + \text{MET})$, as represented on Fig. 6 (left). For the $t\bar{t}$ background, a bound is observed at m_t, whereas for the $\tilde{t}_1\tilde{t}_1^*$ signal it is correlated to $\Delta m(\tilde{t}_1, \tilde{\chi}_1^\pm)$ leading sensitivity to large $\Delta m(\tilde{t}_1, \tilde{\chi}_1^\pm)$ and low $\Delta m(\tilde{\chi}_1^\pm, \tilde{\chi}_1^0)$. In order to set up a selection orthogonal to [18], one requests $m_{T2}(\ell_1, \ell_2, \text{MET})$ <90 GeV and $m_{T2}(b_1, b_2, \ell_1 + \ell_2 + \text{MET}) > 160$ GeV.

Figure 6 (right) presents the exclusion limits at 95% CL in the plane $m_{\tilde{\chi}_1^0}$ versus $m_{\tilde{\chi}_1^\pm}$ combining the two analyses [15, 18].

The search for $\tilde{t}_1 \to b\tilde{\chi}_1^\pm$ with $\tilde{\chi}_1^\pm \to W\tilde{\chi}_1^0$ performed by CMS on events with 1 lepton in the final state [14], makes use of the boosted decision tree technique after a cut on $m_T(\ell, \text{MET}) >$

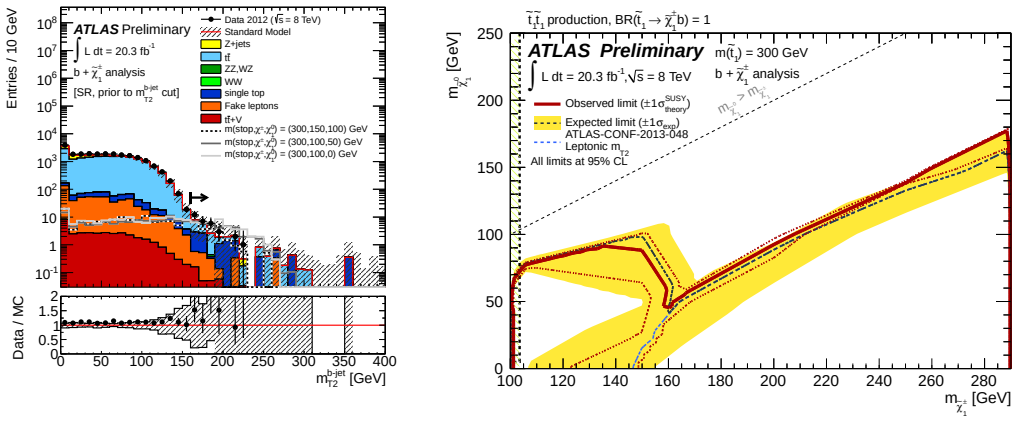

Figure 6: Left: Distribution of $m_{T2}(b_1, b_2, \ell_1 + \ell_2 + \text{MET})$ after selection. SM backgrounds are represented by colored histograms, the bands representing the total uncertainty. Three different models are also shown for comparison. Right: Exclusion limits at 95% CL in plane $m_{\tilde{\chi}_1^0}$ versus $m_{\tilde{\chi}_1^\pm}$ for $m_{\tilde{t}} = 300$ GeV.

120 GeV as defined by Eq. (3). Exclusion limits at 95% CL are presented on Fig. 7 in the $(m_{\tilde{t}_1}, m_{\tilde{\chi}_1^0})$ plane, for different values of the mass parameter x characterizing $m_{\tilde{\chi}_1^\pm} = \text{x} \cdot m_{\tilde{t}_1} + (1 - \text{x}) \cdot m_{\tilde{\chi}_1^0}$. For completeness, a summary of the limits extracted by the different ATLAS analyses, with different $m_{\tilde{\chi}_1^\pm}$ hypotheses, is also displayed on Fig. 7.

7 Study on Polarization

The signal acceptance depends on the polarization of the decay products: the top in the $\tilde{t}_1 \to t\tilde{\chi}_1^0$ mode and the W and $\tilde{\chi}_1^\pm$ in the $\tilde{t}_1 \to b\tilde{\chi}_1^\pm$ mode, which depends on the L/R mixing of the $\tilde{t}_1$ and on the mixing matrices of the $\tilde{\chi}_1^0$ and $\tilde{\chi}_1^\pm$. Based on events selected with 1 lepton in the final state ("1-lepton channel"), the variations on the exclusion limits obtained by CMS when varying the polarization are displayed on Fig. 8 [14]. This study has also been performed by ATLAS for the $\tilde{t}_1 \to t\tilde{\chi}_1^0$ mode for a fixed mass of the $\tilde{\chi}_1^0$ [17]. Unlike the 1-lepton channel, the $\tilde{t}_1 \to t\tilde{\chi}_1^0$ search in the 0-lepton channel is insensitive to the top polarization [16].

8 Study on the Branching Ratio

All the SUSY analyses present now their results in the context of SMS, with a BR of 100%. Limits for smaller BR can be extrapolated from the $\tilde{t}_1 \to t\tilde{\chi}_1^0$ results assuming that the analysis is only sensitive to this mode, as it is shown on Fig. 9 for CMS (left) [14] and ATLAS (right) [16], for example if the $\tilde{\chi}_1^\pm$ and $\tilde{\chi}_1^0$ are nearly mass-degenerated (i.e. with a mass parameter x∼0).

For larger mass differences ($m_{\tilde{\chi}_1^\pm} > m_{\tilde{\chi}_1^0}$), a conservative approximate cross section limit can be obtained as $\sigma(pp \to \tilde{t}_1\tilde{t}_1^*) < min\left[\sigma_0/B^2, \sigma_+/(1-B)^2\right]$ where σ_0 (σ_+) is the cross section limit for the 100% $\tilde{t}_1 \to t\tilde{\chi}_1^0$ ($\tilde{t}_1 \to b\tilde{\chi}_1^\pm$) scenario and $B = \text{BR}(\tilde{t}_1 \to t\tilde{\chi}_1^0)$.

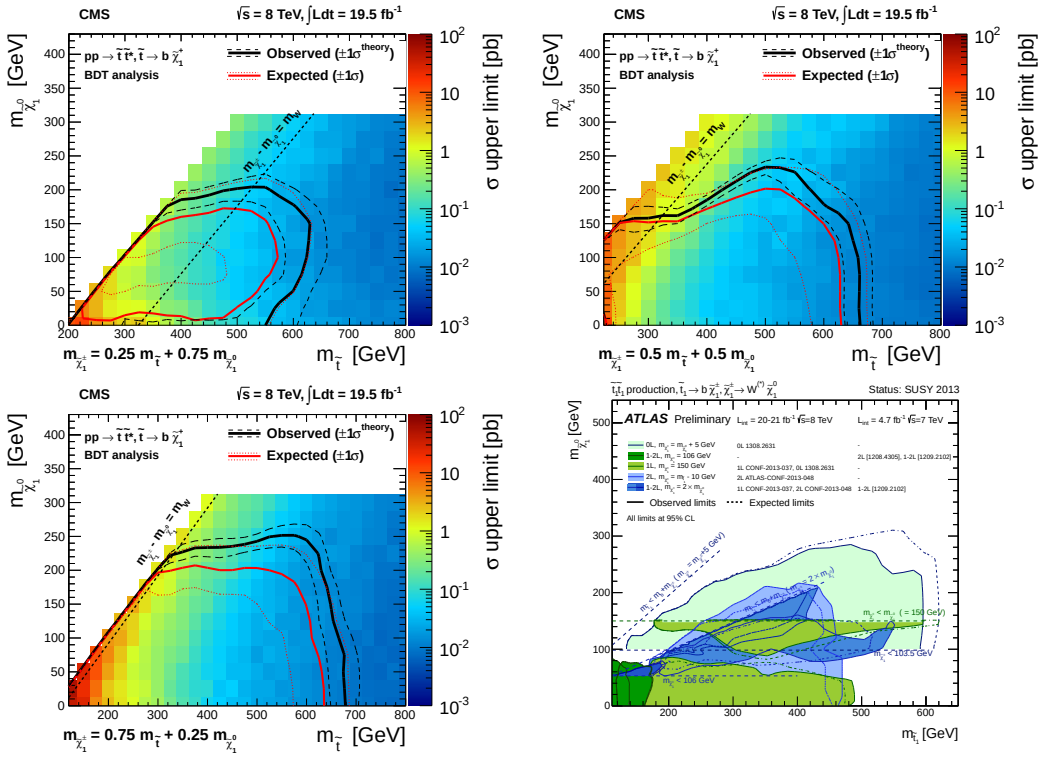

Figure 7: Exclusion limits at 95% CL for the $\tilde{t}_1 \to b\tilde{\chi}^{\pm}$ process as a function of $m_{\tilde{t}_1}$ and $m_{\tilde{\chi}_1^0}$ for a mass parameter of (top left) x=0.25, (top right) x=0.5 and (bottom left) x=0.75 used by CMS (the color scale indicates the observed cross section upper limit), and (bottom right) for different $m_{\tilde{\chi}_1^{\pm}}$ hypotheses by ATLAS.

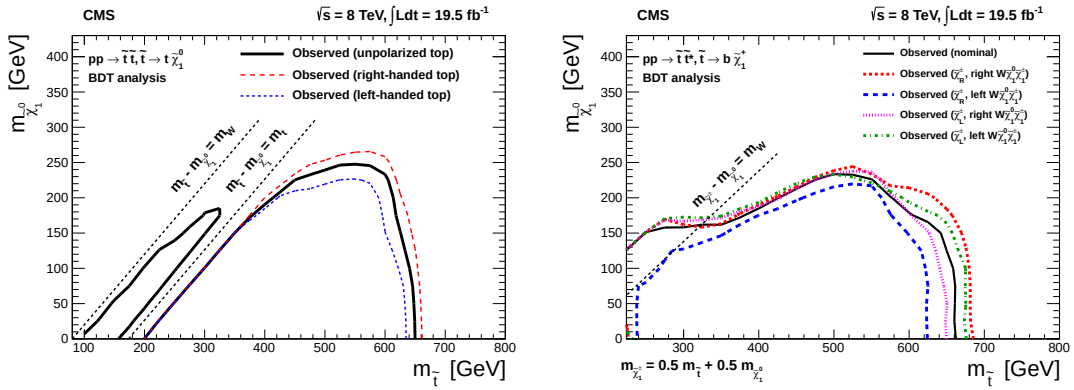

Figure 8: Effect of the polarization on the observed excluded regions in the 1-lepton channel. Left: For the $\tilde{t}_1 \to t\tilde{\chi}_1^0$ mode, limits are displayed for unpolarized, right-handed and left-handed t quarks. Right: For the $\tilde{t}_1 \to b\tilde{\chi}_1^\pm$ mode with x=0.5, the nominal scenario is compared to right-handed vs. left-handed $\tilde{\chi}_1^\pm$ ($\tilde{\chi}_R$ and $\tilde{\chi}_L$, respectively), and right-handed vs. left-handed $W\tilde{\chi}_1^0\tilde{\chi}_1^\pm$ couplings.

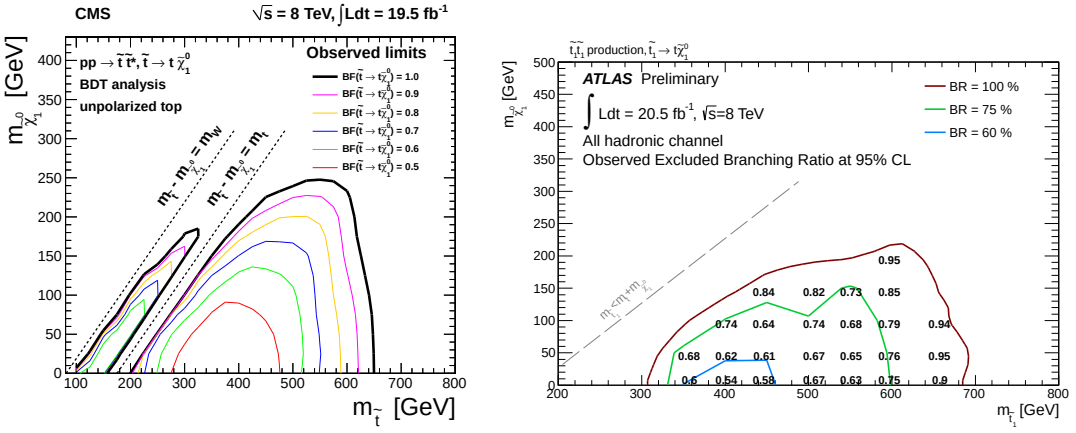

Figure 9: Observed excluded region as a function of BR($\tilde{t}_1 \to t\tilde{\chi}^0$) for CMS (left) and ATLAS (right), assuming that the analysis has no acceptance to other decay modes.

9 Conclusions

Natural SUSY motivates the search for light squarks of third generation. The ATLAS and CMS Collaborations address the question of $\tilde{t}_1$ and $\tilde{b}_1$ through several analyses, covering different decay modes with different signatures and techniques. The latest results have been discussed here. There are still work ongoing in order to cover more and more phase space. For example, the kinematical region where $\Delta m(\tilde{t}_1, \tilde{\chi}_1^0) \sim m_t$ is hardly accessible by direct $\tilde{t}_1$ pair production, but some exclusion limits can however be extracted with the $\tilde{t}_2 \to \tilde{t}_1 Z$ channel [19]. More SUSY scenarios are also investigated, like $\tilde{t}_1$ searches in RPV [20] or in GMSB [19, 21, 22]. Let us hope that with next LHC run, we will not continue to set up further limits but rather discover the first signs of SUSY.

Acknowledgments

C. Collard has received support from the Agence Nationale de la Recherche (ANR-12-JS05-002-01 BATS@LHC).

References

[1] M. Kramer, A. Kulesza, R. van der Leeuw, M. Mangano, S. Padhi, T. Plehn and X. Portell, arXiv:1206.2892 [hep-ph].

[2] G. Aad *et al.* [ATLAS Collaboration], JINST **3** (2008) S08003.

[3] S. Chatrchyan *et al.* [CMS Collaboration], JINST **3** (2008) S08004.

[4] G. Aad *et al.* [ATLAS Collaboration], JHEP **1310** (2013) 189, arXiv:1308.2631 [hep-ex].

[5] T. Aaltonen *et al.* [CDF Collaboration], Phys. Rev. Lett. **105** (2010) 081802, arXiv:1005.3600 [hep-ex].

[6] V. M. Abazov *et al.* [D0 Collaboration], Phys. Lett. B **693** (2010) 95, arXiv:1005.2222 [hep-ex].

[7] CMS Collaboration, CMS PAS SUS-13-013.

[8] ATLAS Collaboration, ATLAS-CONF-2013-007.

[9] ATLAS Collaboration, ATLAS-CONF-2013-068.

[10] V. M. Abazov *et al.* [D0 Collaboration], Phys. Lett. B **665** (2008) 1, arXiv:0803.2263 [hep-ex].

[11] T. Aaltonen *et al.* [CDF Collaboration], JHEP **1210** (2012) 158, arXiv:1203.4171 [hep-ex].

[12] LEPSUSYWG, ALEPH, DELPHI, L3 and OPAL experiments, note LEPSUSYWG/04-01.1.

[13] CMS Collaboration, CMS PAS-SUS-13-004.

[14] S. Chatrchyan *et al.* [CMS Collaboration], Eur. Phys. J. C **73** (2013) 2677, arXiv:1308.1586 [hep-ex].

[15] ATLAS Collaboration, ATLAS-CONF-2013-065.

[16] ATLAS Collaboration, ATLAS-CONF-2013-024.

[17] ATLAS Collaboration, ATLAS-CONF-2013-037.

[18] ATLAS Collaboration, ATLAS-CONF-2013-048.

[19] ATLAS Collaboration, ATLAS-CONF-2013-025.

[20] S. Chatrchyan *et al.* [CMS Collaboration], Phys. Rev. Lett. **111** (2013) 221801, arXiv:1306.6643 [hep-ex].

[21] CMS Collaboration, CMS PAS SUS-13-002.

[22] CMS Collaboration, CMS PAS SUS-13-014.